PHILOSOPHICAL TRANSACTIONS OF THE ROYAL SOCIETY A MATHEMATICAL, PHYSICAL & ENGINEERING SCIENCES

The Earth's Core and the Phase Diagram of Iron

O. L. Anderson

Phil. Trans. R. Soc. Lond. A 1982 **306**, 21-35
doi: 10.1098/rsta.1982.0063

Phil. Trans. R. Soc. Lond. A **306**, 21–35 (1982) [21]
Printed in Great Britain

The Earth's core and the phase diagram of iron

By O. L. Anderson
Institute of Geophysics and Planetary Physics,
University of California at Los Angeles,
Los Angeles, 90024, *U.S.A.*

The phase diagram of iron is presented for $P \leqslant 330$ GPa. The melting curve is derived from Stevenson's generalized form of Lindemann's law, successfully connecting the low-pressure (5–20 GPa) measurements to the new shock-wave measurements of 250 GPa. The isothermal equation of state of ε-iron (h.c.p.) and γ-iron (f.c.c.), indicate that the inner core density is that of pure solid iron. The present experiments cannot distinguish between the ε or γ phase for the inner core, but preference is given to γ-iron.

From these constructions, it is concluded that the melting temperature of iron at the inner core – outer core boundary pressure, $T_{\mathrm{m}}^{\mathrm{i}}$ (i.c.b.), is 5200–6600 K. A likely model of the outer core temperature is presented by taking 5800 K as the probable value of $T_{\mathrm{m}}^{\mathrm{i}}$ (i.c.b.), and assuming a temperature drop of 1000 K due to chemically induced melting point depression. This yields 3620 K for the T of the core side of the core–mantle boundary (c.m.b.). This model results in a large $\Delta T(\mathrm{D}'')$, (700 K), at the c.m.b., but the shock-wave data also allow other models where $\Delta T(\mathrm{D}'')$ is less. A numerical experiment reveals that the value for $\Delta T(\mathrm{D}'')$ of 700 K does not lead to distortion of the density profile.

The (γ–ε–liquid) triple point is beyond the i.c.b. Thus, diluted γ-iron in the liquid phase constitutes the outer core. The experiments support a thermally driven model of the geomagnetic dynamo, and further support a model of a slowly freezing inner core for the energy source.

Introduction

Recent reports by Brown & McQueen (1980, 1982) on the measurement of the melting point and the ε–γ phase transition of iron by shock waves has resolved a number of questions on the phase diagram of iron, strengthened some current ideas about the chemical composition of the Earth's core, and constrained estimates of the temperature profile.

They measured the longitudinal wave velocity, v_{l}, along the iron Hugoniot and found the pressure where v_{l} converged to the bulk sound velocity, c_{b}. From the Hugoniot data, the temperature of the transition was computed. They reported their measurement of the fusion temperature $T_{\mathrm{m}}(P)$ of iron on the Hugoniot to be 5000–6000 K at 250 ± 10 GPa. In addition they found a solid–solid transition by an abrupt decrease of v_{l} along the Hugoniot at 200 ± 2 GPa. They reported the temperature to be 4400 ± 300 K. The primary laboratory data are shown in figure 1.

These two high-pressure transition measurements can be connected with the static high-pressure measurements of iron taken below 20 GPa, where the phase diagram of iron is completely known. The dynamic measurements thus place limits on the melting temperature of iron at a pressure corresponding to that of the inner–outer core boundary, $T_{\mathrm{m}}^{\mathrm{i}}$(i.c.b.) (the superscript refers to iron).

† Publication no. 2284, Institute of Geophysics and Planetary Physics, University of California, Los Angeles, California 90024 (USA).

Brown & McQueen (1982) (hereafter cited as B. & M.) estimate T_m^i(i.c.b.) to be 6200 ± 500 K from the shock-wave results. They have also reported the data for density, ρ, against P (up to 200 GPa) for the ε-iron isotherm (300 K). The implications of these measurements on current chemical and thermal models of the Earth's core will be discussed in this paper.

Perhaps the most important conclusion of these experiments is that T_m^i(i.c.b.) thus obtained is much higher than many reported values. In particular, the experimental results exclude the values of T_m^i(i.c.b.) based upon the Kennedy law (Kraut & Kennedy 1966) where T_m is presumed to be a linear function of the change in volume, $\Delta V/V_0$. The shock experiments clearly show that T_m plotted against $\Delta V/V_0$ for iron is not a straight line but is concave upwards. Simon's theory of melting (Simon 1953) gives values of T_m^i(i.c.b.) that are much too low. Thus the original form of the Simon eq uation is excluded by the experimental results.

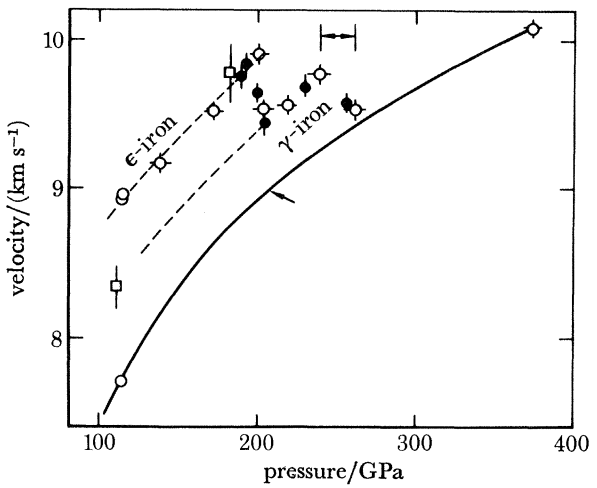

FIGURE 1. Elastic wave velocities as a function of pressure along the Hugoniot of iron, as presented by Brown & McQueen (1982). The solid line is the calculated bulk sound velocity. ●, Two-stage gun experiments; ○, explosive experiments; □, Al'tshuler (1971). (Reproduced by permission of M. Brown.)

The early version of the Lindemann theory (1910) predicts values outside the experimental range. However, a generalized form of the Lindemann law, deduced from liquid-state theory (Stevenson 1980, 1981) satisfies the data as shown below.

A second important result from these experiments is that the γ phase is in equilibrium with the liquid at all outer core pressures (135–330 GPa).

A third important result is that agreement is found between the density values of γ-iron at inner core conditions and the density of the inner core as given by seismic models.

A fourth important result is that the temperature jump at the core–mantle boundary may be as large as 700 K.

From these results the temperature profile of the Earth is constructed. The experiments support the thermal model where heat production and magnetization is produced largely by the equilibrium steady freezing of the core.

THE EARTH'S INNER CORE

There can be little doubt that both the inner and outer cores of the Earth are predominantly iron with the inner core solid and the outer core liquid. Birch (1952) argued successfully in his classic paper that iron is alloyed with some lighter element in the core because the density of

pure iron is higher than the density of the core. Since that time, the nature and distribution of the alloying element(s) has been a matter of contention.

Verhoogen (1961) proposed that slow cooling and crystallization of the core, accompanied by a corresponding growth of the inner core, provides the heat necessary for convection in the outer core. This is analogous to metallurgical processing with fractional crystallization by a moving solid–liquid interface. In any solid where the solute depresses the freezing point, and the solidus is distinguishable from the liquidus, the solute concentration in the freezing solid is lower than that of the liquid (Pfann 1958). A slowly moving inner core boundary (*ca.* 1 cm/year) is analogous to a long bar undergoing equilibrium freezing. Here the solute concentration in both solid and liquid is uniform, and the concentration in the solid is k_0 times that of the liquid, where k_0 is the equilibrium distribution coefficient ($k_0 < 1$) of the solute.

Thus, Verhoogen's idea amounts to assuming that the solute concentration in the liquid is many times more than in the solid, the ratio depending upon k_0 at core pressures. If the inner core is growing, we can expect there to be a marked compositional difference between the inner and the outer cores (Masters 1979). Ahrens (1980) observed: '... it appears that the inner core... may be composed of pure iron', a conclusion resulting from his shock-wave experiments.

Jeanloz (1979) analysed all the existing iron shock-wave data including porous samples and computed the thermodynamic properties of iron at core conditions. He found that it is plausible that the 'inner core does in fact consist of solid iron, and that the inner–outer core boundary represents not only a phase... but a compositional boundary.'

In this section, I present additional evidence that the inner core can be modelled as pure iron. The approach is to use the reduced shock-wave data on the ε phase of solid iron taken up to 200 GPa, to define an equation of state (e.o.s.) that is used to extrapolate the density to inner-core conditions (326–363 GPa).

The 300 K isothermal P–ρ data set for the ε-iron phase reported by B. & M. was deduced from the Hugoniot data, limited by the 200 GPa transition. These data agree quite well with the static compression data on ε-iron reported by Mao & Bell (1979), which extended to 1 00 GPa. The parameters ρ_0 and K_0, reported by B. & M., will be used here.

Two popular e.o.s's in geophysical literature were used to compute the density of iron at pressures within the inner core and are used below: the Morse potential (M–P) e.o.s. and the Zarkov & Kalinin (Z–K) exponential e.o.s. A discussion of these e.o.s's and their properties is found in Stacey *et al.* (1981; see their equations (96) and (90)).

The parameters used for ε-iron are (B. & M.):

$$\rho_0 = 8.28 \text{ g cm}^{-3};$$

$$K_0 = 178.2 \text{ GPa}.$$

For M–P, $K_0' = 5.2$ and for Z–K, $K_0' = 4.8$. These values for the e.o.s's were chosen to reproduce the ε-iron data at the highest measurements of the solid in the ε phase. The computed density is shown in figure 2. The values for ρ_0 and K_0 for ε-iron can be compared with those measured on α-iron (Guinen & Beshers 1968), where $\rho_0 = 7.873$ and $K_0 = 166.4$ GPa. It is seen that both ρ_0 and K_0 increase from the α to the ε phase in accord with general principles of modulus–density systematics. The volume diminishes by 0.075 cm^3 mol^{-1} from α to γ at zero pressure (Birch 1972); e.g. the density of γ phase should be close to 7.91. $K_0 = 167$ GPa was found by using the same proportionality constant for the K ratio as the ρ ratio. The value for K_0' for the γ phase was found by requiring the density at 110 GPa (the α–γ–ε triple point)

to be such that ΔV (ε–γ) = 0.18 cm³ mol⁻¹, as reported by Liu (1975). Thus $K_0' = 5.51$ in the γ phase in the M–P e.o.s. and 4.8 in the Z–K e.o.s. By using these three parameters for γ-iron, the density was calculated at core pressures for the two e.o.s's and plotted in figure 2.

A value of 34–40 GPa for the thermal pressure, P_{th}, was used for finding temperature corrections to the density at the inner core i.c.b. (see calculations in the next section). The density distribution on the 300 K isotherm was shifted to core conditions by adding P_{th} to P. The density of the ε phase is thus estimated to be 13.5–14.0 g cm⁻³ and the density of the γ phase is 13.0–13.4 g cm⁻³ at inner core conditions. The γ phase computed density lies between the density distribution of the CAL8 model (Bolt 1980) and the PEM model (or the PREM model) (Dziewonski *et al.* 1975; Dziewonski & Anderson 1981). (Note, however, that both phases have densities substantially higher than the QM_2 model (Jordan & Anderson 1974).) It appears that γ-iron satisfies the existing density of the inner core obtained by the latest seismic models, whereas ε-iron is somewhat more dense than either of the seismic models.

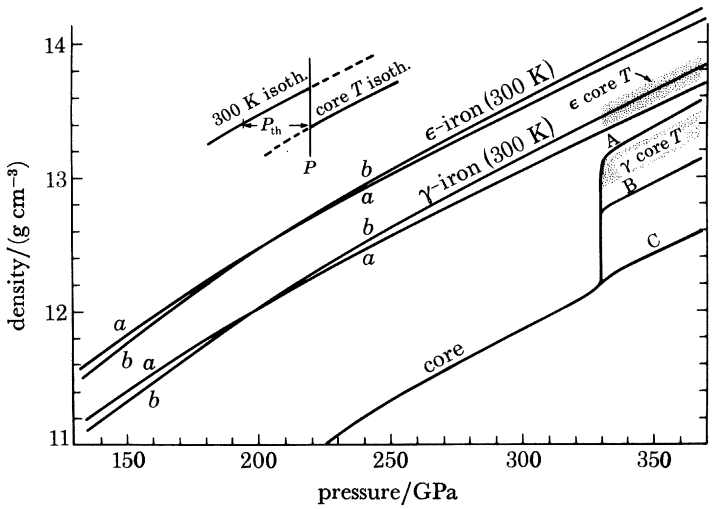

FIGURE 2. The density profile of ε- and γ-iron at 300 K plotted against P, in comparison with the density profile of the core. Two standard e.o.s's are used to construct the profiles at core temperatures. The density profiles of ε- and γ-iron are quite close to the CAL8 (A) and the PREM (B) seismic models. C, QM_2; *a*, Zharkov–Kalinin e.o.s.; *b*, Morse potential e.o.s.

Solutes appear to be necessary for the inner core only if the seismic model selected has a minimal $\Delta\rho$ at the i.c.b. (such as QM_2). In any case, there can be only a slight concentration of solute in the inner core, based upon the assumption that the core is slowly cooling. If the solutes are either sulphur or oxygen, k_0 is quite small, as described below.

The fact that pure solid iron e.o.s. parameters satisfy the inner core density profile means that the inner core's concentration of Ni can probably be neglected in physical calculations. To add Ni to a pure iron inner core would require the addition of a corresponding light solute to counterbalance the effect that Ni has on increasing the density (McQueen & Marsh 1966).

Traditionally, the inner core has been assumed to be a Ni–Fe alloy because of the observed Ni–Fe compounds in meteorites. However, Brett (1976) pointed out that the analogy of the Earth's core and Fe–Ni meteorites is based in part upon an incorrect assumption. Brett (1971) previously reported that if one uses cosmic abundance arguments, the whole core should contain about 4% Ni by mass. Traditional geophysical estimates of nickel content have been higher than 4%.

Several authors have noted (see Bolt, this symposium) that the Poisson ratio of the inner core is large. A value for σ of 0.44 for an iron inner core is quite reasonable because of pressure effects. This results from the fact that the shear velocity increases less rapidly with pressure than the longitudinal velocity, a consequence of lattice structure. The effect is especially pronounced for NaCl and CsCl structures (Anderson & Demarest 1971), and for f.c.c. structures (Falzone & Stacey 1980).

The outer core

The shock-wave results described above require γ-iron to be in equilibrium with the liquid at outer core conditions. As shown in figure 2, the density of γ-iron at core temperature in comparison with the outer core indicates that $\Delta\rho$(i.c.b.) = 1.00 g cm^{-3} (including the ΔV between γ and the liquid phase). This agrees with the reduced shock-wave data, which suggest that $\Delta\rho$(i.c.b.) is between 5 and 12% (B. & M.; Stevenson 1981; Ahrens 1980). This range of $\Delta\rho$(i.c.b.) is much larger than that obtained by a phase change alone. Masters (1979) reports $\Delta\rho$(i.c.b.) = 0.05 g cm^{-3} and Verhoogen finds $\Delta\rho$(i.c.b.) = 0.06 g cm^{-3} for a solid–liquid phase change. Thus a compositional boundary must account for nearly all $\Delta\rho$(i.c.b.) although there is a remote possibility that the ε–γ phase change could account for part of it. If $\Delta\rho$(i.c.b.) is due to a compositional boundary, the solutes lower the γ-iron density by about 0.95 g cm^{-3}. This $\Delta\rho$ permits an easy calculation of a chemically induced lowering of the melting temperature at the i.c.b. if two assumptions can be justified: (1) ideal mixture of solute and solvent; (2) small concentrations of solute. There is some contention on whether these assumptions can be justified (see B. & M. (1982) and Verhoogen (1980) for arguments for and against).

If these assumptions can be justified, the depression of the melting point is related only to the solute concentration as evidenced by the density jump but is independent of exact knowledge of the solute. Such calculations indicate that $\Delta T_m \approx 1000$ K for $\Delta\rho \approx 1.0$ g cm^{-3}. Stevenson (1981) suggested that $\Delta T_m \approx 1000$ K for $\Delta\rho \approx 1.0$ g cm^{-3}. In any case, the concentration of solute is smaller than a eutectic composition (Stevenson 1981). This means that the depression in T_m is essentially controlled by the concentration of the solute. All in all, it appears that $\Delta\rho$(i.c.b.) is *ca.* 1.0 g cm^{-3} (see Bolt, this symposium). Stevenson's results suggest that ΔT_m(i.c.b.) = 1000 K (Stevenson 1981).

To go further, the solutes must be specified. The physical arguments for and against a particular solute rely heavily on shock-wave experiments and their interpretations, especially the work of Ahrens (1980). Further work on this subject is presented by him in an accompanying paper in this volume. Candidate solutes must also satisfy a number of geochemical restrictions. These have been reviewed by Jacobs (1975), Brett (1976) and Ringwood (1977). Favourite candidates for core solutes are oxygen (as FeO), S, MgO and Si, the first two being the leading contenders.

Stevenson (1980) made a convincing case for the major solute in the outer core to be sulphur. He also pointed out that the outer core is not a simple chemical system: '...the combined effect on the density of small amounts of Si, C, N, MgO and H may be comparable to or greater than the effect of S or O_2'.

Another point should be made in support of S and O_2 as temperature depressants. These impurities in iron have much smaller equilibrium distribution coefficients, k_0, than many others such as Si. Hayes & Chipman (1939) derived the following values of k_0 in an iron host:

sulphur, 0.05; oxygen, 0.10; silicon, 0.66; manganese, 0.84. This means that at $P = 0$ there should be only one twentieth as much S in the solid as in the liquid near the interface. Simonsen & Dossin (1965) confirmed essentially these results by zone refining experiments. Effects of pressure on k_0 are not known, but it is plausible that at core pressures both S and O are efficiently concentrated in the outer core, leaving the inner core significantly depleted in these elements.

Physical properties of the outer core should be related to liquid state theory, as emphasized by Verhoogen (1980) and Stevenson (1980). Outer core properties estimated from properties of solid iron or from solid-state equations will be received with suspicion. Unfortunately, the experimentally determined properties of liquid iron are known only at very low pressures. Therefore, liquid-state theory needs to be invoked at high pressures.

Stevenson (1980) derived two equations from liquid theory valid at high P and near T_m that are important to e.o.s's and melting theory:

$$dK/dP = 5 - 5.6\,P/K \tag{1}$$

(which neglects a small term due to thermal energy), and

$$\frac{d \ln T_m^i}{dP} = \frac{1}{K}\frac{2(C_V^{vib}\gamma - R)}{2C_V^{vib} - 3R}, \tag{2}$$

where C_V^{vib} is the lattice vibrational contribution to the heat capacity, γ is the thermodynamic Grüneisen ratio, and R is the gas constant. Neither C_V^{vib} nor γ include electronic corrections.

Equation (2) is the liquid state equivalent of Lindemann's law, and reduces to it exactly within the classical limit $C_V^{vib} = 3R$. Grover (1971) has shown that in general C_V^{vib} is not equal to $3R$ at T_m for liquid metals.

The constants in (2) must now be evaluated as a function of P. The density of liquid iron at $P = 0$ is 7.00 g cm^{-3} at 1868 K (*CRC Handbook*). The velocity of sound in liquid iron at atmospheric pressure is 4.4 km s^{-1} according to Filipov *et al.* (1966) (a smaller value is given by Kurz & Lux (1969)); coupled with the density, this gives $K_0 = 133$ GPa.

The liquid iron $K(P)$ distribution is found by joining the seismic $K(P)$ distribution curve for the outer core with K_0 of liquid iron. This distribution represents approximately adiabatic conditions. The density of liquid pure iron will be higher than the liquid iron mixed with solutes, but provided that the outer core is well mixed, the depression of the freezing point does not have any effect on comparisons of adiabatic and melting gradients (Jamieson *et al.* 1978).

Stacey & Irvine (1977) derived an equation analogous to (2) by using a thermodynamic theory starting from the Clausius–Clapeyron equation:

$$(1/T_m^i)\,(dT_m^i/dP) = (1/K)\,[2(\gamma - 2\gamma^2\epsilon)] \tag{3}$$

The term containing ϵ arises from a thermal expansivity correction, $\epsilon = \alpha T_m^i$, and will be a small percentage of γ. Equations (2) and (3) thus answer the objection of many that Lindemann's law is based only upon properties of the solid state.

Equation (2) is used for the calculations because data exist on C_V^{vib} at T_m for metals (Grover 1971). The value for γ for core conditions must be specified. Unfortunately the literature on high pressures lists widely differing values for γ. A few of these estimates are listed in table 1. In general, γ(i.c.b.) < γ(c.m.b.).

In this paper four cases are considered, each of which represents one of the current views on appropriate γ values. They are:

$$(a)\ \gamma(\text{c.m.b.}) = 1.6,\quad \gamma(\text{i.c.b.}) = 1.4;$$
$$(b)\ \gamma(\text{c.m.b.}) = 1.4,\quad \gamma(\text{i.c.b.}) = 1.2;$$
$$(c)\ \gamma(\text{c.m.b.}) = 1.2,\quad \gamma(\text{i.c.b.}) = 1.0;$$
$$(d)\ \gamma(\text{c.m.b.}) = 1.1,\quad \gamma(\text{i.c.b.}) = 0.9.$$

TABLE 1. ESTIMATES OF γ AND $\bar{\gamma}$ FOR IRON AT PRESSURES CORRESPONDING TO THE INNER–OUTER CORE BOUNDARY (I.C.B.) AND THE CORE–MANTLE BOUNDARY (C.M.B.)

($\bar{\gamma}$ includes a correction for the electronic contribution.)

	γ		$\bar{\gamma}$	
	c.m.b.	i.c.b.	c.m.b.	i.m.b.
Stacey (1977)	—	—	1.32	1.17
Boschi & Mulargia (1977)	—	—	1.3	0.73–0.93
Jamieseon *et al.* (1978)	1.2–2.0	1.2–2.0	1.2–2.0	1.2–2.0
Welch *et al.* (1978)	1.15	1.04	—	—
Anderson (1979)	1.45–1.65	1.4–1.6	—	—
Jeanloz (1979)	—	—	1.4	1.0
Stevenson (1981)	—	—	1.7	1.6
this paper	1.1–1.3	0.9–1.1	—	—
(probable)	(1.2)	(1.0)	(1.3)	(1.1)

Case (*a*) is close to the values recommended by Stevenson (1980, 1981). Case (*b*) is close to the γ values used by Stacey (1977) and by Boschi & Mulargia (1977).

Integration of (2) was justified up to 330 GPa because through this pressure range there are no electronic transitions for γ-iron (Bukowinski & Knopoff 1976).

It turns out that the integration of (2) produces values for $T_{\mathrm{m}}^{\mathrm{i}}$ much higher than the B. & M. results at 250 GPa if $C_V^{\mathrm{vib}} = 3R$.

Agreement with experiment was secured by assuming C_V^{vib} to be larger than $3R$. This was justified in view of the experimental evidence gathered by Grover (1971) showing that C_V^{vib} for several metals has a wide cusp at T_{m}, in which the specific heat rises substantially above $3R$. Such a cusp is consistent with an order–disorder transformation. The value used in the calculation was $C_V^{\mathrm{vib}} = 3.5\,R$.

Integration of (2) requires an estimate of γ at all pressures. The $P = 0$ value of γ is 2.44 according to Stevenson (1981). However, the integration begins at the (γ–δ–l) triple point, where $P = 5.2$ GPa. Here $T_{\mathrm{m}}^{\mathrm{i}}(5.2) = 1991$ K and $\mathrm{d}T_{\mathrm{m}}^{\mathrm{i}}/\mathrm{d}P = 40$ K GPa^{-1} (Strong *et al.* 1973), from which $\gamma(5.2) = 1.81$ calculated from (2). Smooth empirical curves were drawn between $\gamma(5.2)$ and the appropriate set, γ(c.m.b.) and γ(i.c.b.), from which values were interpolated for intermediate pressures.

The integration of (2) leads to $T_{\mathrm{m}}^{\mathrm{i}}(P)$ curves for the four cases shown in figure 3. Case (*a*) is above the experimental range at 250 GPa reported by B. & M. Cases (*b*) and (*d*) bracket the estimated measurements of Brown & McQueen (1980), and case (*c*) intercepts the mid-point of their error bars.

We see that the Lindemann law in the liquid-state generalization (Stevenson 1980) works very well for iron because it joins the lower pressure measurements of Strong *et al.* (1973) with the shock-wave measurements of B. & M. This constitutes a verification of Stevenson's liquid-state version of the Lindemann theory. The extrapolated values for T_{m} at the i.c.b. are

5200–6600 K, but also substantiates the estimate of B. & M. with a probable value taken to be 5800 K.

The thermodynamic version of the Lindemann theory (Stacey & Irvine 1977) also satisfies the data provided that the $2\gamma^2\epsilon$ term in (3) is taken to be about 10% of γ and varies in an appropriate manner with depth.

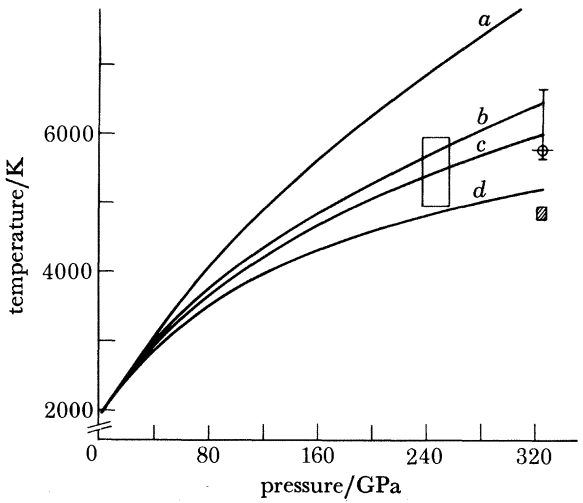

FIGURE 3. The fusion curve of pure iron for several sets of values of the Grüneisen parameter, γ. Three models satisfy the shock-wave data of Brown & McQueen (1980, 1982) shown by the box. Case C (▨) is used in subsequent calculations. *a*, γ = 1.6–1.4; *b*, γ = 1.3–1.1; *c*, γ = 1.2–1.0; *d*, γ = 1.1–0.9.

TABLE 2. PREDICTED TEMPERATURES AT THE INNER–OUTER CORE BOUNDARY (I.C.B.) PRESSURE AND AT THE CORE–MANTLE BOUNDARY (C.M.B.)

(T at c.m.b. based upon ΔT_m = 1000 K due to temperature depression by light elements.)

iron melting (i.c.b.), T_m/K		core side of c.m.b. in the Earth, T/K	
Bundy & Strong (1962)†	6400–8100	Alder (1966)	4400
Higgens & Kennedy (1971)	4250	Birch (1972)	< 4000
Birch (1972)	5100	Stacey (1977)	3157
Lappaluto (1972)	7000–9000	Jeanloz & Richter (1979)	3000
Boschi (1975)‡	6600	Brown & Shankland (1981)	2505
Liu (1975)	5125	Brown & MacQueen (1980)	3700–4200
Boschi *et al.* (1979)‡	4500–7000	Stevenson (1981)	3200
Abelson (1981)§	7800	Anderson & Baumgardner (1981)	3492
Stevenson (1981)	6300	Stacey *et al.* (1981)	3770
Brown & MacQueen (1982)¶	5700–6700	Anderson (1981)	3131
this paper	5200–6600	this paper	3220–3720
(probable)	(5800)	(probable)	(3620)

† Based upon an extrapolation from experiments at 6 GPa.
‡ A special case of the Ross theory (1969).
§ Based upon Monte Carlo theory.
¶ Based upon an extrapolation from experiments at 250 GPa.

The values of T_m^i at core–mantle boundary pressures are more contained because of the lower spread of values at 135 GPa: T(c.m.b.) = 4350 ± 250 K.

Case (*c*) in figure 3, where T_m^i(i.c.b.) = 5800 K and T_m^i(c.m.b.) = 4400 K, bisects the Brown & McQueen error limits at 250 GPa. Comparisons of this result with others in the literature are given in table 2.

To estimate the temperature of the outer core one subtracts the ΔT due to solute depression. Stevenson (1981) suggests that ΔT(i.c.b.) $= -1000$ K for a $\Delta\rho$ 1.0 g cm^{-3}. If this ΔT is adopted, T_m^{oc}(i.c.b.) = 4200–5600 K, and the recommended probable value is T_m^{oc}(i.c.b.) = 4800 K. It is close to the value suggested by B. & M., but lower because of the low slope, dT_m/dP, found in this model.

To find the temperature of the outer core, an adiabat is passed through the T_m^{oc}(i.c.b.) point following the law

$$(\partial T/\partial P)_s = \bar{\gamma}T/K. \tag{4}$$

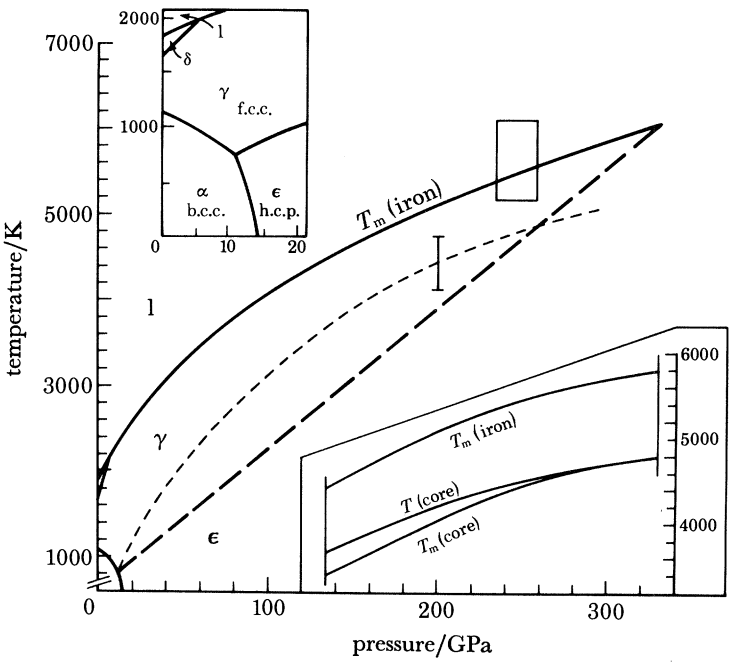

FIGURE 4. The phase diagram of iron from case C of figure 3 for the fusion curve. The inset shows the construction of the fusion curve and the temperature of the outer core. The two broken lines show outside possibilities for the ε–γ phase boundary.

This $\bar{\gamma}$ includes electronic effects and should be slightly larger than γ. Following Stacey (1977) and Jamieson *et al.* (1978), adding a small term to γ is equivalent to the detailed calculation, so $\bar{\gamma} = \gamma + 0.1$ was assumed. The adiabat appropriate to case (*c*) is found by integration of (4) from the point T_m^{oc}(i.c.b.) = 4800 K, P = 329 GPa. This gives the recommended probable value T^{oc}(c.m.b.) = 3620 K. This model of the temperature profile of the outer core is plotted as the insert in figure 4. The shock wave data allow T^{oc}(c.m.b.) to be as low as 3220 °K, assuming ΔT(i.c.b.) = 1000 °K due to solute depression.

The value of T/T_m varies from 1.02 to unity throughout the outer core. This means that C_V^{vib} is everywhere larger than $3R$ in the outer core, since the cusp in C_V^{vib} at the liquid transition is more than 2% (Grover 1971). I take C_V^{vib} to be 3.5 R throughout the outer core.

The value of $(\partial P/\partial T)_V$ can be calculated from the classic Grüneisen relation

$$(\partial P/\partial T)_V = \alpha K_t = \gamma C_V/V. \tag{5}$$

C_V has a contribution from electrons. Following Jamieson *et al.* (1978), the electronic contribution is about one-half the classical limit. Thus $C_V = 4.5\,R$. This gives $\alpha K_t = 0.007$ GPa K^{-1}

approximately throughout the outer core from case, (*c*). Thus αK is virtually independent of depth (Birch 1952; Anderson & Sumino 1980; Baumgardner & Anderson 1981). From the equations for K_s/K_t and αK_t, $\alpha = 1.1 \times 10^{-5}$, $K_t = 610$ GPa for $K_s = 634$ at the c.m.b., and $\alpha = 5.0 \times 10^{-6}$, $K_t = 1277$ GPa for $K_s = 1277$ at the i.c.b. The equation of the thermal pressure at high temperature is given approximately by Anderson (1980, 1982) as

$$P_{th} = b + (\alpha K_t)\, T.$$

At core temperatures b can be neglected: $P_{th} = 25$ GPa at the c.m.b. and 34 GPa at the i.c.b. The anharmonic lattice contribution could be 0–5 GPa, giving $P_{th} = 34$–40 GPa at the i.c.b. P_{th}(i.c.b.) was used to compute the displacement of the ε- and γ-iron isotherms at core temperatures from the 300 °C isotherm (see figure 2).

The temperature at the Earth's centre is found by using the value $\gamma = 1.87$ found by Bukowinski (1977), and applying (4). This yields $T_c = 4980$ K.

Thus our best probable temperature values coincide with the upper limit of Birch's judgement (1972) that 'estimates of 4000 K for the core mantle boundary, and 5000 K for the central temperature...may have some standing as upper limits'.

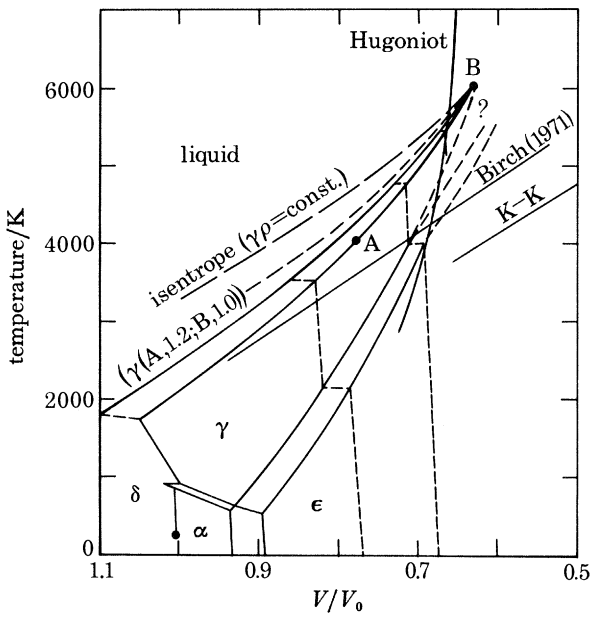

FIGURE 5. The phase diagram of iron in T–V/V_0 space (following Birch 1972). The phase boundaries are concave upward, unlike the linear law used by Birch. The Kraut–Kennedy line for iron is shown. B is the i.c.b. pressure and A is the core–mantle boundary pressure. The two broken lines are isobars at 100 and 250 GPa.

THE (γ–ε–l) TRIPLE POINT

It is apparent from the measurements of B. & M. that the ε–γ phase line, if drawn straight between their measurements and the (α–ε–γ) triple point (t.p.), intersects the liquidus just below the i.c.b.

If the t.p. was at a P below the i.c.b., a disturbance in the density curve is expected because of the difference between ρ of the γ and ε phases there. However, there is no evidence of such a disturbance, judging from the behaviour of Bolt & Bullen's homogeneity index. Bolt & Uhrhammer (1981) report the index of homogeneity to be constant out to the i.c.b., and further

report that the boundary is quite sharp. Masters (1979) reports that the liquid region next to the i.c.b. appears not to be stratified. The (γ–ε–l) t.p. should occur below the i.c.b.

The t.p. may occur either at a P found in the inner core, or greater. Resolution of a density jump large enough to accommodate the ε–γ transition at inner core pressures may not be resolvable by seismic models. Bolt (this symposium) gives evidence that the inner core may have distinct regions. Thus the triple point could occur in the inner core, but there appears to be no way to check this.

Birch (1972) constructed two hypothetical phase diagrams in P–V space, assuming T_m to be linear in $\Delta V/V_0$. One case was for the t.p. to occur at 400 GPa, beyond the Earth's central pressure, and the other was for the t.p. at 100 GPa. Liu (1975) estimated the t.p. to be at even lower pressures.

Birch's first case is closer to the experimental results, although the occurrence of t.p. right at the i.c.b. is not excluded. A hypothetical construction of the phase diagram in P–V space, using the results above but following Birch's method of construction, is presented in figure 5.

If the t.p. occurs near the i.c.b., the slope $\Delta T/\Delta P$ for the α–γ_1 transition has to be virtually constant over the whole pressure range. This requires ΔS to diminish at the same rate as ΔV, from the Clausius–Clapeyron equation. In many solids, phase line slopes are constant, but in these the compression is small compared with that of iron. A constant slope for the ε–γ phase line over such a large compression is possible but unlikely. Theoretical considerations indicate that for the B_1–B_2 transition in alkali halides, ΔS is proportional to $(\Delta v)\, v_1$, where V_1 is the volume of phase 1 (Jeanloz 1982). Moreover, $\Delta T/\Delta P$ becomes negative before ΔV vanishes (Bassett *et al.* 1968).

The question for the iron ε–γ transition is, does ΔS decrease as ΔV, or is it more like the case of the alkali halides, where ΔS decreases as $(\Delta v)\, v_\varepsilon$? In the latter case, $\mathrm{d}T/\mathrm{d}P$ would be monotonically decreasing with P and the inner core would definitely by γ-iron. Liu (1975) reports that $\Delta V(\gamma\text{–}\varepsilon) = 0.18\ \mathrm{cm^3\ mol^{-1}}$ at the (α–ε–γ) t.p. (110 GPa) and B. & M. report about $0.05\ \mathrm{cm^3\ mol^{-1}}$ at 200 GPa. Thus ΔV appears to be decreasing rapidly with P, and is probably very small at the i.c.b. pressure.

Two extreme possibilities for the γ–ε transition line are shown as broken lines in figure 4, the upper by using the low pressure slope for $\mathrm{d}T/\mathrm{d}P$ reommended by Liu (1975), 30 K $\mathrm{GPa^{-1}}$, and the lower found by Takahashi & Bassett (1964), 20 K $\mathrm{GPa^{-1}}$. All in all, the case for the inner core to be constituted of γ-iron is more favoured.

The temperature profile at the core–mantle boundary

Consider the lowest possible value of T_m^i(c.m.b.) allowed by the fusion curve defined by the B. & M. shock wave results: 4100 K. Consider also that the chemically induced ΔT by solutes is 1000 K, as suggested by Stevenson (1981), yielding T_m^{oc}(c.m.b.) = 3150 K and T^{oc}(c.m.b.) = 3270 K. Is this consistent with the temperature profile of a periodotite mantle?

Since peridotite has olivine as a major constituent, T can be fixed at the beginning of the transition zone (380 km). The T of the modified spinel transition in olivine is 1670 K (Akaogi & Akimoto 1979). Thus T(380 km) = 1670 K.

Various phase changes through the transition zone, from further results of Akaogi & Akimoto (1979), gives T(670 km) = 1830 K (Baumgardner & Anderson 1981). This agrees with estimates of the acoustic properties of the high-pressure phases of olivine at this P and T

TABLE 3. VARIATION OF DENSITY (ρ), TEMPERATURE (T), PRESSURE (P), GRAVITY, BULK MODULUS (K), dK/dP, COEFFICIENT OF THERMAL EXPANSION (α) AND RESIDUAL MOMENT OF INERTIA RATIO (I/I_0) WITH DEPTH FOR SPHERICALLY SYMMETRIC EARTH

radius / km	depth / km	ρ / g cm^{-3}	ρ/ρ_0	T / °C	gravity / cm s^{-2}	ρ / GPa	K / GPa	dK/dP	α / MK^{-1}	I/I_0
6371	0	1.030	1.000	5	982.0	0.00	100.0	0.0	0.0	1.000
6368	3	1.030	1.000	5	982.7	0.03	100.2	5.00	0.0	0.999
6368	3	2.800	1.000	5	982.7	0.03	70.0	0.0	24.27	0.999
6360	11	2.798	0.999	171	983.3	0.25	69.7	−0.60	24.38	0.996
6360	11	2.898	0.999	171	983.3	0.25	69.7	0.0	24.38	0.995
6350	21	2.898	0.999	329	983.9	0.54	69.8	0.61	24.35	0.991
6350	21	3.357	0.993	329	983.9	0.54	123.3	0.0	40.54	0.991
6320	51	3.339	0.988	653	984.8	1.52	120.0	−3.41	41.68	0.974
6280	91	3.316	0.981	1082	986.2	2.84	115.5	−3.40	43.29	0.952
6271	100	3.310	0.979	1177	986.5	3.13	114.5	−3.39	43.67	0.947
6271	100	3.310	0.979	1177	986.5	3.13	114.5	0.0	43.67	0.947
6250	121	3.328	0.984	1195	987.3	3.82	117.7	4.71	42.47	0.935
6200	171	3.368	0.996	1235	989.1	5.47	125.5	4.68	39.84	0.910
6150	221	3.406	1.008	1275	991.0	7.15	133.3	4.66	37.50	0.884
6100	271	3.444	1.019	1314	992.8	8.85	141.2	4.63	35.41	0.859
6050	321	3.480	1.030	1352	994.6	10.57	149.1	4.59	33.53	0.834
6000	371	3.516	1.040	1389	996.5	12.31	157.1	4.58	31.83	0.810
5950	421	3.550	1.050	1426	996.4	14.07	165.1	4.55	30.28	0.787
5950	421	3.765	1.043	1426	998.4	14.07	188.1	0.0	26.59	0.787
5900	471	3.831	1.051	1454	999.3	15.96	200.5	6.55	24.93	0.762
5850	521	3.897	1.059	1480	1000.1	17.89	213.1	6.43	23.47	0.738
5800	571	3.962	1.066	1506	1000.8	19.86	225.7	6.38	22.15	0.714
5750	621	4.027	1.072	1532	1001.4	21.86	238.4	6.32	20.98	0.691
5700	671	4.092	1.079	1557	1001.9	23.89	251.1	6.19	19.91	0.668
5700	671	4.391	1.044	1707	1001.9	23.89	303.4	0.0	21.43	0.668
5600	771	4.450	1.058	1757	1000.2	28.32	316.6	3.01	20.53	0.621
5400	971	4.564	1.085	1855	997.3	37.32	343.2	2.91	18.94	0.535
5200	1171	4.675	1.112	1949	994.9	46.52	370.1	2.90	17.56	0.459
5000	1371	4.784	1.138	2040	993.6	55.92	397.3	2.86	16.36	0.392
4800	1571	4.890	1.163	2128	993.5	65.53	424.8	2.87	15.30	0.334
4600	1771	4.995	1.188	2214	995.2	75.36	452.7	2.80	14.36	0.283
4400	1971	5.098	1.212	2298	999.2	85.42	481.0	2.82	13.51	0.240
4200	2171	5.199	1.236	2381	1005.1	95.74	509.8	2.78	12.75	0.203
4000	2371	5.300	1.261	2461	1015.7	106.36	539.3	2.78	12.05	0.172
3800	2571	5.401	1.284	2541	1031.9	117.31	569.4	2.79	11.42	0.145
3600	2771	5.502	1.309	2619	1053.1	128.67	600.5	2.73	10.82	0.125
3485	2886	5.561	1.322	2664	1068.6	135.42	618.9	2.67	10.50	0.115
3485	2886	9.883	1.435	3364	1068.6	135.42	614.7	0.0	8.13	0.115
3400	2971	10.019	1.454	3427	1050.0	144.38	647.9	3.71	7.72	0.102
3200	3171	10.319	1.498	3564	1003.9	165.27	724.9	3.66	6.90	0.077
3000	3371	10.591	1.538	3690	954.8	185.76	800.0	3.64	6.25	0.057
2800	3571	10.839	1.574	3805	903.1	205.68	872.7	3.63	5.73	0.041
2600	3771	11.065	1.506	3910	849.1	224.86	942.5	3.63	5.31	0.029
2400	3971	11.269	1.636	4006	793.1	243.22	1009.0	3.64	4.96	0.019
2200	4171	11.454	1.563	4092	735.3	260.60	1071.8	3.59	4.67	0.013
2000	4371	11.621	1.587	4171	676.0	276.89	1130.5	3.61	4.42	0.008
1800	4571	11.770	1.709	4241	615.6	292.00	1184.9	3.63	4.22	0.005
1600	4771	11.903	1.728	4303	554.6	305.86	1234.7	3.60	4.05	0.003
1400	4971	12.019	1.745	4358	493.5	318.40	1279.7	3.57	3.91	0.001
1215	5156	12.114	1.759	4403	437.7	328.80	1316.9	3.63	3.80	0.001
1215	5156	12.760	1.595	4403	437.7	328.80	1413.2	0.0	5.66	0.001
1200	5171	12.767	1.596	4406	432.5	329.63	1416.4	3.76	5.65	0.001
1000	5371	12.855	1.507	4446	361.6	339.82	1455.7	3.90	5.50	0.000
800	5571	12.926	1.516	4479	289.7	348.23	1488.2	3.85	5.38	0.000
600	5771	12.981	1.523	4504	216.5	354.79	1513.5	3.86	5.29	0.000
400	5971	13.020	1.527	4521	140.5	359.46	1531.5	4.22	5.22	0.000
200	6171	13.041	1.530	4531	48.9	362.02	1541.4	3.86	5.19	0.000
0	6371	13.043	1.530	4532	0.0	362.24	1542.2	0.0	5.19	0.000

PHILOSOPHICAL TRANSACTIONS OF THE ROYAL SOCIETY A MATHEMATICAL, PHYSICAL & ENGINEERING SCIENCES

(Graham & Dobrzykowski 1976). Thus a ΔT of 1790 K must be accommodated between 670 and 2880 km.

The adiabatic change of T across the lower mantle, ΔT_s, has been estimated by various authors. The reported values for $\Delta T_s(D')$ are 662 K (Anderson 1979), 600 K (Stacey 1977), 576 K (Brown & Shankland 1981), 460 K (Jeanloz & Richter 1979) and 760 K (Baumgardner & Anderson 1981). Taking the maximum value above for $\Delta T_s(D')$, a residual ΔT of 680 K has to be assigned to superadiabaticity and thermal boundaries.

It is recognized that for a highly viscous convecting homogeneous body, the temperature is slightly superadiabatic. The superadiabaticity in the lower mantle may accommodate another 200 K, according to Brown & Shankland (1981). A smaller amount, 100–150 K, was estimated by Jeanloz & Richter (1979). Taking the larger value assign $\Delta T_{\text{n.a.}}(D') = 200$ K for superadiabaticity and distributing it evenly throughout the lower mantle leaves 850 K to assign to a temperature jump, $\Delta T(\text{D}'')$, at the core–mantle boundary, D″. Thus a plausible case can be constructed in which the temperature jump at the c.m.b. is small. Taking the recommended value of $T^{\text{oc}}(\text{c.m.b.}) = 3620$ K (see figure 3) and the same value for the chemically induced ΔT at the i.c.b., $\Delta T(\text{D}'')$ is closer to 930 K. Verhoogen (1980) has suggested that the chemically induced ΔT at the i.c.b. may be less than 100 K (perhaps 500 K), in which case $\Delta T(\text{D}'')$ might approach 1450 K.

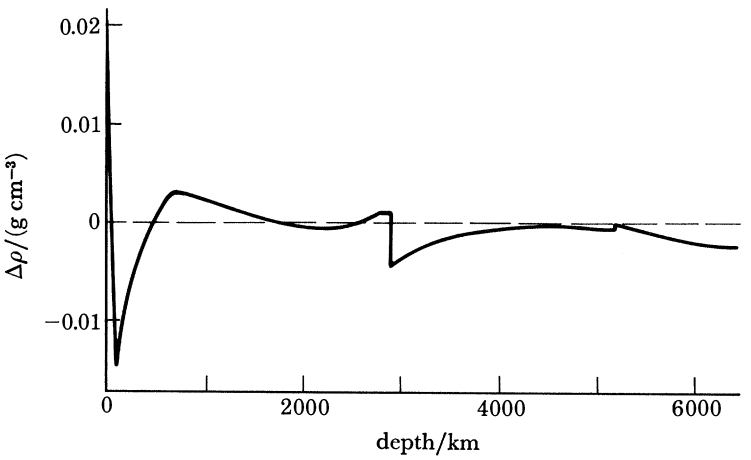

FIGURE 6. The difference, $\Delta\rho$, between the density profile of the Baumgardner & Anderson model, assuming $\Delta T(\text{c.m.b.}) = 700$ K and using the equation of state parameters presented here, and the density profile of the PEM.

The thickness of D″ is close to 100 km, as reported by Bolt & Uhrhammer (1981), so that the thermal gradient of D″ varies between extremes of 5 and 14 K km^{-1}, with the probable value near 9 K km^{-1}. The larger estimates of the gradient agree with the calculations of Jones (1977) and imply that the geomagnetic dynamo is thermally driven.

I considered the question of if an 850 K discrepancy is accounted for in thermal boundaries, could the resulting thermal profile of the core still be consistent with the basic properties of Earth; in particular, its moment of inertia and mass, and the density profile of the mantle. This was checked by using the model of Baumgardner & Anderson (1981) where a set of differential equations is defined for the mechanical and thermal structure of the Earth. These

PHILOSOPHICAL TRANSACTIONS OF THE ROYAL SOCIETY A MATHEMATICAL, PHYSICAL & ENGINEERING SCIENCES

include the e.o.s., the mass and moment of inertia, hydrostatic equilibrium, heat conduction, and heat convection. The solution of these equations gives values for T, P, ρ, α, K, $\mathrm{d}K/\mathrm{d}P$ and g at each depth. The program used the peridotite model for the mantle, and the 850 K was distributed between two thermal boundaries so that $\Delta T(\mathrm{D}'') = 700$ K and $\Delta T(670) = 150$ K. In this model, P, ρ and T are totally dependent upon the boundary conditions. Seismological data are not used to determine the e.o.s. parameters or the density profile.

Temperature was integrated from the surface, and the resulting temperature profile and density profile are listed in table 3. The e.o.s. parameters of the core were adjusted so that the moment of inertia vanished at the centre, resulting in temperatures of the Earth's inner core slightly below those shown in figure 3. Nevertheless, the temperature profile is close to that of case (*c*) and within the limits set by the shock wave results.

The resulting values for ρ tracked the density profile of the PEM (Dziewonski *et al.* 1975) quite well (see figure 6). The resulting values for $\mathrm{d}K/\mathrm{d}P$ in the outer core are near 3.6, agreeing with (1). The moment of inertia and residual mass go to zero at the surface. I therefore conclude that $\Delta T(\mathrm{D}'') = 700$ K is a possible solution. Further numerical experiments showed that the $\Delta T(\mathrm{D}'')$ can be as much as 1000 K without excessive distortions of the density profile.

I thank John Baumgardner for the programming and Frances Raiken for checking the calculations. I am grateful to Dr Michael Brown for an advance copy of his unpublished paper. I profited from comments by Professor Dave Stevenson, Professor John Verhoogen and Professor Bruce Bolt. I wish to acknowledge the long-term support of Dr Eugene Poncelet. Part of the work was done while I was a consultant at the Lawrence Livermore National Laboratory. The major part was supported by the National Sciences Foundation grant no. EAR-7911212.

References (Anderson)

Abelson, R. S. 1981 Ph.D. thesis, University of Calfornia at Los Angeles.
Ahrens, T. J. 1979 *J. geophys. Res.* **84**, 985–998.
Ahrens, T. J. 1980 *Science, Wash.* **207**, 1035–1040.
Akaogi, M. S. & Akimoto, A. 1979 *Phys. Earth planet. Inter.* **19**, 31–51.
Alder, B. J. 1966 *J. geophys. Res.* **71**, 4973–4980.
Al'tshuler, L. V., Brazhnik, M. I. & Telgin, G. J. S. 1971 *J. appl. Mech. tech. Phys.*, pp. 921–926.
Anderson, O. L. 1979 *Phys. Earth planet. Inter.* **18**, 221–231.
Anderson, O. L. 1980 *Phys. Earth planet. Inter.* **22**, 173–183.
Anderson, O. L. 1981 In *Evolution of the Earth* (ed. R. J. O'Connell & W. S. Fyfe), pp. 19–28. Washington, D.C.: American Geophysical Union.
Anderson, O. L. & Baumgardner, J. 1981 *Adv. Space Res.* **1**, 159–176.
Anderson, O. L. 1982 *Phys. Earth planet. Inter.* (In the press).
Anderson, O. L. & Demarest, H. 1971 *J. geophys. Res.* **76**, 1349–1369.
Anderson, O. L. & Sumino, Y. 1980 *Phys. Earth planet. Inter.* **23**, 319–331.
Bassett, W. A., Takahashi, T., Mao, H. K. & Weaver, J. S. 1968 *J. appl. Phys.* **39**, 319–325.
Baumgardner, J. R. & Anderson, O. L. 1981 In *Advances in space physics research* (ed. H. Stiller & R. Z. Sagdeev), vol. 1, pp. 159–176. Pergamon Press.
Birch, F. 1952 Elasticity and composition of the Earth's interior. *J. geophys. Res.* **57**, 227–286.
Birch, F. 1972 *Geophys. Jl Res. astr. Soc.* **29**, 373–387.
Bolt, B. 1964 *Bull. seism. Soc. Am.* **54**, 191.
Bolt, B. 1980 *Annali Geofis.* **30**, 3–4.
Bolt, B. & Uhrhammer, R. A. 1981 In *Evolution of the Earth* (ed. R. J. O'Connell & W. S. Fyfe), pp. 28–29. Washington, D.C.: American Geophysical Union.
Boschi, E. 1975 *Riv. nuovo Cim.* **5**, 501–531.
Boschi, E. & Mulargia, F. 1977 *J. Geophys.* **43**, 465–472.

PHILOSOPHICAL TRANSACTIONS OF THE ROYAL SOCIETY A MATHEMATICAL, PHYSICAL & ENGINEERING SCIENCES

Boschi, E., Mulargia, F. & Bonafede, M. 1979 *Geophys. Jl R. astr. Soc.* **58**, 201–208.
Brett, R. 1971 *Geochim. cosmochim. Acta* **35**, 203–225.
Brett, R. 1976 *Rev. Geophys. Space Phys.* **14**, 375–383.
Brown, E. & McQueen, R. G. 1980 *Geophys. Res. Lett.* **7**, 533–536.
Brown, E. & McQueen, R. G. 1982 In *High pressure research in geophysics* (ed. A. Akimoto & M. Manghnani). Tokyo: Center for Academic Publication. (In the press.)
Brown, M. & Shankland, T. 1981 *Geophys. J.* **66**, 579–596.
Bukowinski, M. S. T. 1977 *Phys. Earth planet. Inter.* **14**, 333–334.
Bukowinski, M. S. T. & Knopoff, L. 1976 *Geophys. Res. Lett.* **3**, 43–48.
Bundy, F. P. & Strong, H. M. 1962 In *Solid state physics* (ed. F. Seitz & D. Turnbull), vol. 13, pp. 81–143. Academic Press.
Dziewonski, A. M. & Anderson, D. L. 1981 *Phys. Earth planet. Inter.* **25**, 297–356.
Dziewonski, A. M., Hales, A. L. & Lapwood, E. R. 1975 *Phys. Earth planet. Inter.* **10**, 12–48.
Falzone, A. J. & Stacey, F. D. 1980 *Phys. Earth planet. Inter.* **21**, 371–377.
Filipov, S. I., Kazov, N. B. & Pronin, L. A. 1966 *Izv. vȳssh. ucheb. Zaved. chevn. Metall.* **9**, 8–14.
Graham, E. K. & Dobrzykowski, D. 1976 *Am. Miner.* **61**, 549–559.
Grover, R. 1971 *J. chem. Phys.* **55**, 3435–3441.
Gubbins, D. 1981 In *Evolution of the Earth* (ed. R. J. O'Connell & W. S. Fyfe), pp. 53–58. Washington, D.C.: American Geophysical Union.
Guinen, M. W. & Beshers, D. N. 1968 *J. Phys. Chem. Solids* **36**, 541–549.
Hayes, A. & Chipman, J. 1939 *Trans. Am. Inst. Min. mrtall. Engrs* **135**, 85–90.
Higgens, G. & Kennedy, G. C. 1971 *J. geophys. Res.* **76**, 1870–1878.
Jacobs, J. A. 1975 *The Earth's core*. New York: Academic Press.
Jamieson, J., Demarest, H. H. & Schiferl, D. 1978 *J. geophys. Res.* **83**, 5929–5935.
Jeanloz, R. 1979 *J. geophys. Res.* **84**, 6059–6069.
Jeanloz, R. 1982 In *High pressure research in geophysics* (ed. A. Akimoto & M. Manghnani). Tokyo: Center for Academic Publishing. (In the press.)
Jeanloz, R. & Richter, F. M. 1979 *J. geophys. Res.* **84**, 5497–5504.
Jones, J. M. 1977 *J. geophys. Res.* **82**, 1703–1709.
Jordon, T. H. & Anderson, D. L. 1974 *Geophys. Jl R. astr. Soc.* **36**, 411–419.
Kraut, E. A. & Kennedy, G. C. 1966 *Phys. Rev.* **451**, 668–675.
Kurz, W. & Lux, B. 1969 *High Temp. – high Press.* **1**, 387–399.
Kuskov, O. L. 1981 In *Evolution of the Earth* (ed. R. J. O'Connell & W. S. Fyfe), pp. 196–209. Washington, D.C.: American Geophysical Union.
Leppaluoto, D. A. 1972 *Phys. Earth planet. Inter.* **6**, 175–181.
Lindemann, F. A. 1910 *Phys. Z.* **11**, 609–612.
Liu, L. 1975 *Geophys. Jl R. astr. Soc.* **43**, 697–705.
Liu, L. & Bassett, W. A. 1975 *J. geophys. Res.* **80**, 3277–3282.
Mao, H. K. & Bell, P. M. 1979 *J. geophys. Res.* **84**, 4533–4536.
Mao, H. K., Bennett, W. & Takahashi, T. 1967 *J. appl. Phys.* **38**, 272–276.
Masters, G. 1979 *Geophys. Jl R. astr. Soc.* **57**, 507–534.
McQueen, R. G. & Marsh, S. P. 1966 *J. geophys. Res.* **71**, 1751–1756.
Pfann, W. G. 1958 *Zone melting*. New York: Wiley.
Ringwood, A. E. 1977 *Geochem. J.* **11**, 111–135.
Ross, M. 1969 *Phys. Rev.* **184**, 233–241.
Simon, F. E. 1963 *Nature, Lond.* **172**, 746–747.
Simonsen, B. & Dossin, J. M. 1965 *J. Iron Steel Inst.* **203**, 380.
Stacey, F. D. 1977 *Phys. Earth planet. Inter.* **15**, 341–348.
Stacey, F. D. & Irvine, R. D. 1977 *Aust. J. Phys.* **30**, 631–660.
Stacey, F. D., Brennan, B. J. & Irvine, R. D. 1981 *Geophys. Surv.* **4**, 189–232.
Stevenson, D. 1980 *Phys. Earth planet. Inter.* **22**, 42–52.
Stevenson, D. 1981 *Science, Wash.* **214**, 611–618.
Strong, H. M., Tuft, R. E. & Hannemann, R. E. 1973 *Metall. Trans.* **4**, 2657–2661.
Takahashi, T. & Bassett, W. A. 1964 *Science, Wash.* **145**, 483–486.
Verhoogen, J. 1961 *Geophys. Jl R. astr. Soc.* **4**, 276–281.
Verhoogen, J. 1973 *Phys. Earth planet. Inter.* **1**, 47–58.
Verhoogen, J. 1980 In *Energetics of the Earth*, pp. 51–65. Washington, D.C.: National Academy of Sciences.
Welch, D. O., Dienes, G. J. & Paskin, A. 1978 A molecular dynamical study of the equation of state of solids at high pressure and temperature. *J. Chem. Phys. Solids* **39**, 589–603.

PHILOSOPHICAL TRANSACTIONS OF THE ROYAL SOCIETY A MATHEMATICAL, PHYSICAL & ENGINEERING SCIENCES